Journal of Electronic Research and Application, 2025, Volume 9, Issue 4
http://ojs.bbwpublisher.com/index.php/JERA
ISSN Online: 2208-3510
ISSN Print: 2208-3502

Study on EMC and OTA Anechoic Chamber Compatibility

Yinfeng Zhou, Ming Chen, Yu Tian, Xun Zhou, Pei Shen

Yancheng Quality and Technical Supervision Comprehensive Inspection and Testing Center, Yancheng 224399, China

Abstract: EMC anechoic chamber is used for radiation emission and radiation immunity test, and the wireless performance of products needs to be tested in OTA anechoic chamber. With more and more electronic and electrical equipment with wireless communication function, the rapid construction of a compatible OTA test system in the existing EMC anechoic chamber can save the cost and space of enterprises and third-party laboratories that already have EMC anechoic chamber. In this paper, the OTA test system is built in the existing EMC anechoic room, the ripple calibration test is carried out according to the OTA standard, the TRP and TIS tests are carried out on two test samples with different wireless communication standards, and the test samples are taken to the OTA anechoic room for a comparison test. The comparison between the ripple calibration data and the OTA test data showed that the EMC anechoic chamber could perform OTA test without affecting the original test ability. The data results provide a basis for the implementation of EMC anechoic chamber compatibility upgrade OTA test, and provide reference for further optimization of the compatible test system, reduction of test differences, and the design of anechoic chamber integrating two test functions.

Keywords: EMC; Anechoic chamber compatibility; Ripple calibration; OTA test

Online publication: August 8, 2025

1. Introduction

With the continuous development and gradual implementation of the Internet of Everything, smart home, smart industry, and other fields, more and more electronic and electrical equipment are endowed with wireless communication functions, which makes the demand for wireless performance testing increasing. As an important test method, OTA (over-the-air interface) test can effectively evaluate the performance of wireless products. Generally, TRP (total radiated power) and TIS (Total omnidirectional sensitivity) are used to measure the transmitting and receiving wireless performance of the whole machine. OTA test site is generally laid on all the walls absorbing materials, through these absorbing materials to absorb electromagnetic waves radiated outward, so as to create a kind of electromagnetic wave completely no reflection phenomenon, in order to simulate the vacuum characteristics. This kind of site is mainly used for the measurement of antenna pattern

and target electromagnetic scattering characteristics, which is usually called a microwave anechoic chamber [1]. The development history of OTA microwave anechoic chambers can be traced back to the early 1950s. In the early 1990s, with the introduction of CTIA (Wireless Communication and Internet Association) compliance test standards for consumer wireless products, the application of OTA anechoic chambers in the wireless performance test of the whole machine has been widely promoted, and the number of its constructions is also increasing.

EMC anechoic chamber is used for radiation emission and radiation immunity tests. The industry generally refers to EMC anechoic chamber as EMC anechoic chamber. In this paper, EMC anechoic chamber is used to distinguish it from OTA microwave anechoic chamber. There are two different forms of EMC anechoic chambers in practical applications: half anechoic chamber and full anechoic chamber. The main reason is that the international EMC standards are first formulated in OATS (outdoor open test field) test, and the semi-anechoic chamber is built to simulate this environment, it is in the shielding room on the five walls (except the ground) laying absorbing materials, and laying conductive floor on the ground to simulate the earth's reflection of the radio waves. When the international EMC standards are made in the semi-anechoic chamber test. Full anechoic room, compared with half anechoic room, on the metal ground is also laid absorbing materials. Through manual operation of half anechoic room can generally be half/full conversion to full or half anechoic room. In the 1990s, with the promulgation of CE (European Union compliance) regulations in Europe, requiring listed products to meet the requirements of electromagnetic compatibility, the number of electromagnetic compatibility anechoic chamber constructions began to surge.

At present, more and more electronic and electrical products integrate wireless functions. From the perspective of the overall number of constructions, the EMC anechoic chamber is significantly larger than the microwave anechoic chamber for wireless performance OTA TPR and TIS test. ETSI EN 301908-2 V13.1.1 and EN 301 908-13 V13.2.1 published by the European Union have added OTA test requirements for WCDMA and LTE TRP and TIS, respectively. If a system compatible with the OTA test requirements can be quickly constructed in the existing EMC anechoic chamber, it will help enterprises and third-party laboratories to save a lot of costs and space resources brought by rebuilding the OTA anechoic chamber. It should be pointed out that the test functions of OTA microwave anechoic chamber and EMC anechoic chamber are different. According to CTIA standard, OTA microwave anechoic chamber is verified by ripple test [2], while EMC anechoic chamber is tested by NSA and VSWR [3] in accordance with CISPR 16-1-4 standard. In this study, an EMC anechoic chamber was selected to build an OTA test system, and the feasibility of building an OTA test system and the test differences between the standard OTA anechoic chamber and the OTA anechoic chamber were evaluated.

2. Construction and site calibration of the EMC total anechoic chamber OTA test system

The experience [4,5] of combining OTA microwave anechoic chamber and electromagnetic compatibility anechoic chamber in the industry. The size of the anechoic chamber is relatively large, which is compatible with antenna test and EMC test. The samples of the two test functions are located in different positions of the anechoic chamber, which has high requirements for site and cost. The common method for EMC chamber compatible OTA test TRP and TIS test function is to use the antenna tower used in EMC test, replace the EMC test antenna installed on the antenna tower with the dual polarization antenna of OTA test, or use the single polarization antenna through the antenna tower rotation, vertical polarization, and horizontal polarization. In this paper, the test efficiency

and the error caused by the antenna replacement operation are fully considered, and a worse OTA test scheme is considered to evaluate the feasibility of upgrading the OTA test function of the EMC anechoic chamber. The specific system layout is shown in **Figure 1**.

The field of the OTA test system to be built is the EMC anechoic room, the size of the anechoic room is 8.6m * 4.6m * 4.4m (L*W*H), and the anechoic room includes a program-controlled lifting antenna tower and a horizontal rotating turntable.

The existing hardware in the anechoic room is used to build the OTA test system as shown in **Figure 1**. The test system includes 7 groups of dual-polarization test antennas, RF control unit, 3D turntable, communication antenna, laser positioner, RF cable, etc. The equipment control is connected to the shielded indoor fiber controller through the optical fiber. The test distance of EMC anechoic chamber is generally 3 m or 10 m. Compared with the OTA test antenna replacement method, this method is closer to the test distance. At the same time, the antenna bracket and RF cable are closer to the test static zone, which increases the influence on the OTA test results.

As shown in **Figure 1**, 7 groups of dual-polarized test antennas are arranged at 15° intervals in the area opposite the screen door of the andimatic chamber, forming a 90° test Angle. The test antenna is 1.5 m away from the center of the turntable, and the convenience of installation and the realizability of andimatic chamber fusion are considered while placing as many test antennas as possible. After position measurement and positioning, the 3D turntable was placed on the 2D turntable used for EMC test. The height of the fixed position of the test sample was the center of the height in the anechoic chamber, and the headroom distance in the anechoic chamber was 3 m. Considering the practical handling convenience, the original 2D horizontal turntable of EMC can also be used, combined with the vertical (φ) axis rotation device of the distributed coordinate system, to jointly realize the 360° rotation function of vertical and horizontal axes.

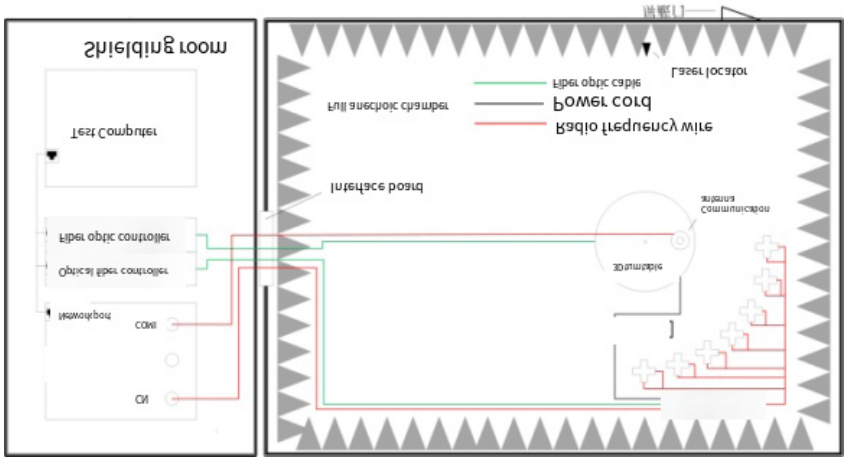

Figure 1. Hardware layout of EMC anechoic chamber OTA test system

The ripple calibration of the test site was carried out according to the requirements of CTIA on the OTA test site. In the test process, considering the electromagnetic compatibility test and layout requirements, the antenna control tower was fixed and located in the original fixed position, and the influence of the antenna tower on the ripple test results was comprehensively considered.

Field test photos are shown in **Figure 2** and **Figure 3**. During the test, the calibration antenna is configured to match a 6 dB attenuator, the RF cable is equidistantly installed with a magnetic ring, and the dynamic range of the

test environment is greater than or equal to 40 dB.

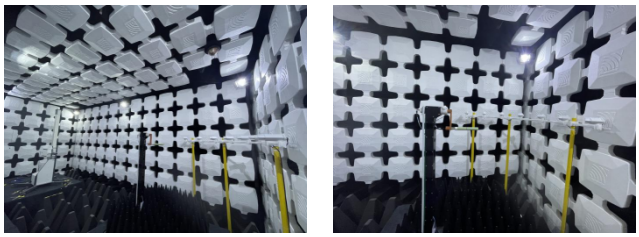

Figure 2. *θ-axis* ripple field test diagram

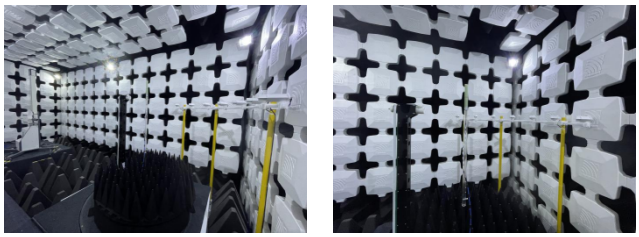

Figure 3. *Field* test diagram of φ-axis ripple

The test antenna is a dipole antenna, including five groups of test antennas, 800 MHz, 1850 MHz, 2500 MHz, 3600 MHz, and 5500 MHz, which basically cover the common low frequency, middle frequency, and high frequency bands of short-range wireless communication and cellular communication. In the calibration process, according to the CTIA standard, the θ axis and φ axis ripple calibration of each antenna were carried out respectively, as shown in **Figure 4**, and 6 and 7 points were tested respectively according to the standard requirements, and the interval between each point was 150 mm±3. Six points were tested on the φ axis, which were (0, -), (0, 0), (0, +), (+, -), (+, 0), (+, +); The θ axis is (0, -, 0), (0, 0, 0), (0, 0, 0), (0, 0, -), (0, 0, +), (+, 0, 0), (-, 0, 0).

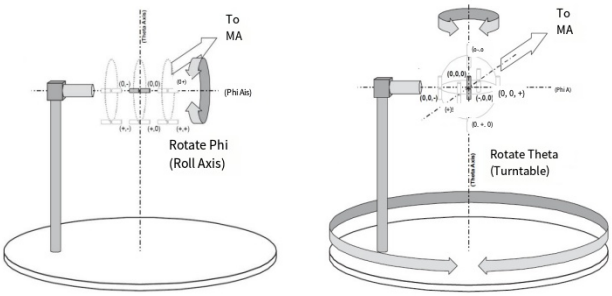

Figure 4. Calibration points and position coordinates of φ *axis* and θ axis of the distributed test system

After the ripple measurement is completed, the data of the 800 MHz dipole antenna ripple test is shown in **Figure 5**. It can be seen from the figure that the data difference between the six different test positions on the φ axis is small, and the test data at each test position is smooth and circular, and the data difference between the seven different test positions on the θ axis is large. The test data of different test positions fluctuated greatly in a specific test Angle interval, and the test data was stable in the test Angle area close to the test antenna.

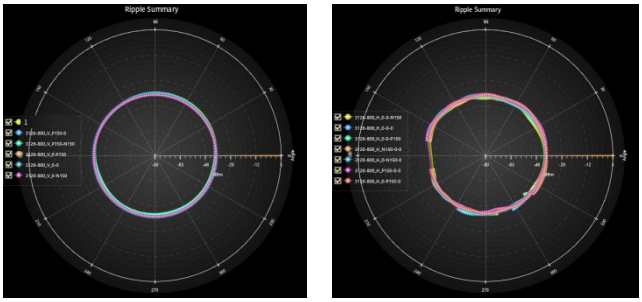

Figure 5. Test data diagram of 3126-800 dipole antenna axis ripple

According to the correlation ripple calculation formula in CTIA, the series power sequence {Pk} is obtained for each measurement position. The standard deviation of each position can be obtained by statistical calculation.

According to Formula 1, the data of all test points at each location are transformed into linear units, that is, the unit of test result power value is transformed into mW.

$$p_k = 10^{p_k(dB/10)}$$

Calculate the spherical standard deviation S () of each position by Eq. 2. P_k

$$s(p_k) = \sqrt{\frac{1}{(N-1)}\sum_{k=0}^{N-1}\left[\left(\left(\frac{p_k}{\overline{p}}-1\right)\sin(\theta_k)\right)^2\right]}$$

According to the standard, the maximum S () in 13 ripple test positions can be taken and put into formula 3 to calculate the standard uncertainty μ in dB. The extended uncertainty can be obtained by multiplying μ by 2. The result is the ripple test result of EMC full anechoic chamber at this frequency. P_k In order to significantly show the ripple test data difference of each test point, the S () of each test point is put into equation 3 in this paper, and the extended uncertainty data of each test position is obtained, as shown in **Table 1** and **Table 2**. P_k

$$u(x) = 10\log\left(1+\max\left(s_j\left(p_k\right)\right)\right)$$

Table 1. φ axis calibration data table

Test position	Dipole antenna frequency (MHz)				
	800	1850	2500	3600	5500
(+,+)	1.50	1.02	1.38	1.45	1.42
(+, 0)	1.43	1.42	1.17	1.64	1.88
(+,-)	1.58	1.58	1.16	1.51	1.68
(0, +)	0.12	0.29	0.23	0.64	0.34
(0, 0)	0.11	0.34	0.24	0.48	0.49
(0 -)	0.12	0.39	0.27	0.42	0.23

Table 2. *Theta* axis calibration data table

Test position	Dipole antenna frequency (MHz)				
	800	1850	2500	3600	5500
(0, 0, +)	1.32	1.71	1.20	0.93	0.66
(0, 0)	1.06	2.27	1.80	1.82	0.78
(0, 0, -)	1.01	2.36	1.53	1.25	1.05
(-, 0, 0)	1.17	1.39	1.05	1.14	0.76
(0, 0, -)	1.58	1.20	0.90	0.59	1.55
(0, 0, +)	1.99	1.42	0.92	0.48	1.07
(0, 0, +)	1.57	1.38	0.74	1.04	1.55

It can be seen in **Table 1** that the ripple test data of (0,+), (0,0), and (0,-) at three positions on the φ axis of the five dipole antennas are relatively small, and the maximum value is only 0.64 dB. The ripple test data of (+,+), (+,0), (+,-) at three positions 150 mm away from the axis of φ are larger, and the maximum value is 1.88, which is 3 times that of the axial line test data, indicating that the maximum extended uncertainty of the φ axis ripple test is caused by the test position 150 mm away from the axis of φ. The maximum spread uncertainty of the five dipole antennas with different frequencies is distributed in the three test points. The influence of the overall test environment on different frequencies is not fixed, but with the increase of frequency, the uncertainty of high frequency is larger. Check to see the circular radar chart of each test antenna, and it can be seen that the fluctuation is large in the specific test Angle interval and gradually presents an ellipse. In the actual test environment, the absorbing foam on the rotating table is inconsistent with the absorbing foam on the top of the anechoic chamber, which may lead to a large uncertainty of φ axis ripple.

According to the experience of CTIA OTA certification, the measurement uncertainty of the whole system will be too high to exceed the requirements [6] of the standard when the measurement is over 1.2 dB. It can be seen in **Table 2** that the ripple spread uncertainty values of the seven positions of the five dipole antennas on the θ axis are relatively large, and the maximum value reaches 2.27 dB, which is much larger than the spread uncertainty of 1.2 dB. The maximum uncertainty test positions of the five antennas are (0,0,0), (+,0,0), (0,0,-), (0,0,+), respectively. These four positions are in the same horizontal plane and close to the calibration test antenna. Due to the size of the site, the distance between the calibration antenna and the absorbing foam of the anechoic chamber is short, and the design information of the anechoic chamber is referenced. It may be that there is not enough space reserved for the calibration antenna and the absorbing foam, which leads to the large [7] uncertainty of the expansion of these positions.

The maximum uncertainty test data of the five dipole antennas are 1.99, 2.27, 1.80, 1.82, 1.55, respectively, and the five data are θ-axis test data, which indicates that the φ-axis ripple test data in the EMC anechoice environment is better than the θ-axis environment, which indicates that the vertical polarization environment of the EMC anechoice is worse than the horizontal polarization environment. In the subsequent improvement process, the uncertainty of horizontal polarization ripple propagation should be optimized first [8]. The maximum spread uncertainty of the five antennas is 2.27 dB, which is 1.07 dB larger than 1.2 dB. In order to meet the overall uncertainty requirements of the system, when the overall size of the EMC anechoic chamber cannot be changed, the distance between the test antenna and the absorbing foam in the anechoic chamber is increased

by adjusting the center position of the turntable. At the same time, the absorbing foam with a better reflection coefficient is replaced on the turntable [9].

3. Comparison of OTA test data in different anechoic chambers

The test samples are one mobile phone and one router, respectively. The test includes the test of Bluetooth, Wi-Fi, GSM, and LTE wireless communication protocols. In the test process, except for the wireless mode tested, other wireless modes are turned off[10]. During the test, the position of the antenna control tower used in the EMC test was fixed and located at the original fixed position. The influence of the antenna tower on the OTA test results was comprehensively considered. The photos of the test site are shown in **Figure 6**.

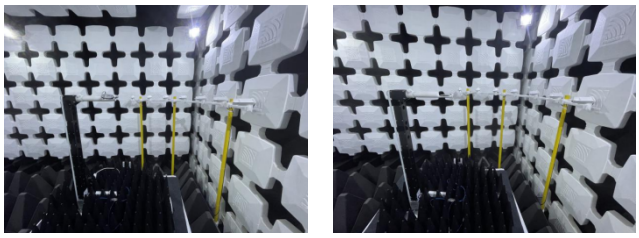

Figure 6. Photos of OTA test in EMC anechoic chamber of test sample

After the TRP test is completed, the test data is shown in **Figure 7**, which includes θ axis, φ axis, and the comprehensive test data. The TRP was tested according to 15° steps, and the whole spherical test point data [11] was measured.

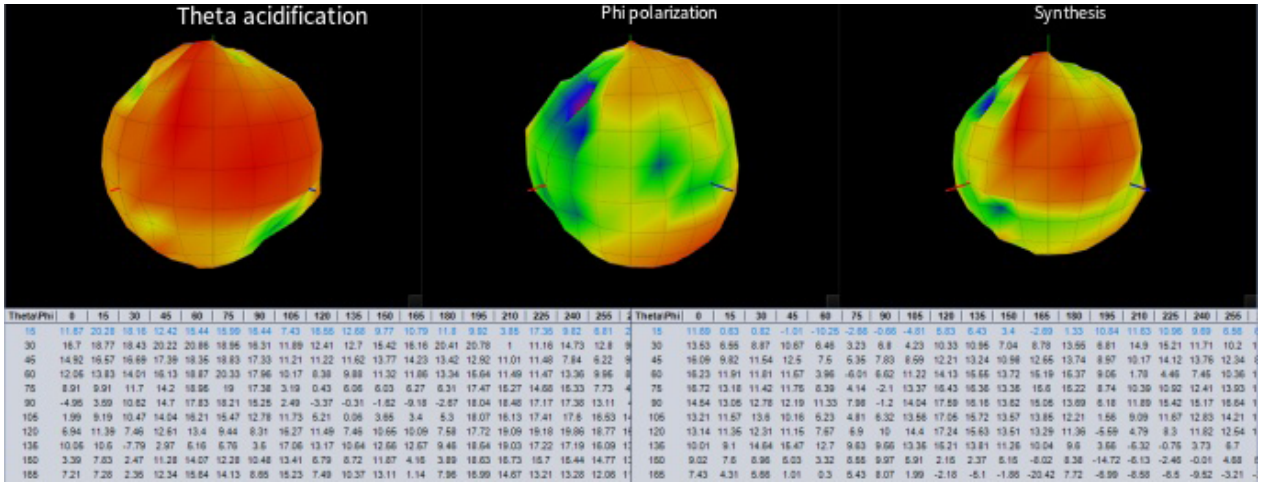

Figure 7. Sample OTA TRP test data

The TIS test method is the same as the TRP test, and the test step is performed at 30° [12]. After the test is completed, the test data of each test point is calculated according to the calculation formula (4) and formula (5) stipulated in the CTIA standard, and the TPR and TIS data are calculated respectively, and the OTA test data in the EMC andimatic chamber shown in **Table 3** can be obtained.

$$TRP \cong \frac{\pi}{2NM}\sum_{i=1}^{N-1}\sum_{j=0}^{M-1}\left[EiRP_{\theta}(\theta_i,\phi_j)+EiRP_{\phi}\left(\theta_i,\phi_j\right)\right]\sin\left(\theta_i\right)$$

$$TIS \cong \frac{2NM}{\pi\sum_{i=1}^{N-1}\sum_{j=0}^{M-1}\left[\frac{1}{EIS_{\theta}\left(\theta_i,\phi_j\right)}+\frac{1}{EIS_{\phi}\left(\theta_i,\phi_j\right)}\right]\sin\left(\theta_i\right)}$$

The test samples were put into the 4 m*4 m*4 m OTA microwave anechoic chamber for TPR and TIS testing, and the working state of the test samples was consistent with the test in the EMC anechoic chamber. Photos of the test site are shown in **Figure 8**.

When this OTA microwave anechoic chamber and another third-party OTA anechoic chamber are tested for capability verification, the test difference is generally 0.5 dB, and the maximum is no more than 1 dB [13].

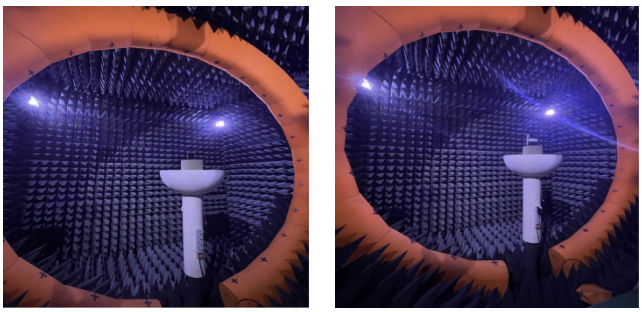

Figure 8. OTA microwave anechoic chamber test diagram of test sample

As shown in **Table 3**, TRP and TIS test data of test samples in EMC anechoic chamber and OTA anechoic chamber were sorted out. In the test process, the Wi-Fi router selected four channels for testing. For mobile phones, one channel was selected for Bluetooth and one channel was selected for Wi-Fi. For GSM, CH 128 and CH 512 were selected. LTE selected CH 42590 for testing [14].

Table 3. Comparison of OTA test data of two anechoic chambers

Test samples	Test channel	TRP		TIS		Difference	
		EMC	OTA	EMC	OTA	TRP	TIS
Road, by device	CH1	14.52	15.98	-90.93	-89.64	-1.46	-1.29
	CH7	14.16	16.03	-88.68	-90.36	-1.87	1.68
	CH13	14.07	14.78	-87.13	-88.69	-0.71	1.56
	CH100	16.02	14.61	-90.49	-91.65	1.41	1.16
	BT_CH40	1.25	2.31	-88.07	-89.12	-1.06	1.05
hand machine	Wi-Fi-CH7	16.38	15.30	-89.34	-87.29	1.08	-2.05
	GSM850	25.80	27.52	-105.21	-105.63	-1.72	0.42
	GSM1900	24.52	23.71	-104.72	-106.71	0.81	1.99
	LTE-B42	16.59	17.66	-93.77	-95.42	-1.07	1.65

The maximum difference of OTA test data between the two anechoic chambers was -1.87 dB to 1.41 dB, the maximum difference of TIS was -2.05 dB to 1.99 dB, the maximum difference of OTA microwave anechoic chamber was ±1 dB, and the OTA test data in EMC anechoic chamber was still about ±1 dB larger than that in OTA microwave anechoic chamber. This data can be compared with the ripple calibration data, and the OTA test data can corroborate the accuracy of the ripple calibration test data.

The extended uncertainty of EMC anechoic chamber ripple calibration data is large at 850 MHz and 1800 MHz dipole antennas. The actual OTA test data show that the largest difference is basically from 2500 MHz and 5500 MHz Wi-Fi test data, except for the GSM 1900 TIS test data. The 3600 MHz band test data can basically be compared with the ripple test data, and the reason for the difference may come from the large amount of test data in the Wi-Fi band. When comparing the Wi-Fi OTA test data separately, it is found that the difference is slightly larger than the ripple calibration spread uncertainty, which may be caused [15] by the uncertainty of other parts of the test system.

4. Conclusion

In this paper, a worst-case EMC anechoic chamber upgrade OTA test method is studied. The ripple calibration data and OTA test comparison data show that the test error and uncertainty increase by ±1 dB, and OTA development exploratory test and pre-test can be carried out when allowed. If it is necessary to meet the ripple and uncertainty test requirements specified by OTA, considering the convenience of building the actual system when the size of the anechoic chamber and the absorber material are fixed, the position of the center of the table and the test antenna are adjusted to reduce the system uncertainty by combining the simulation calculation of the reflection coefficient of the anechoic chamber and absorber material.

Through the test data of this scheme, it can be inferred that the system uncertainty of the method based on the EMC antenna tower, replacing the OTA test antenna to upgrade the compatible OTA test capability, is smaller. In this paper, based on the existing EMC anechoic chamber, the two test functions are considered at the beginning of the construction of the anechoic chamber, which can provide a reference for the design of the anechoic chamber with functional integration.

Funding

Yancheng Science and Technology Bureau (YCBK2023027)

Disclosure statement

The authors declare no conflict of interest.

References

[1] Takahashi, Masanori, Suzuki, et al., 2006, High Speed System for Measuring Electromagnetic Field Distribution (Electromagnetic Compatibility (EMC)). ICE Transactions on Communications, 2006.

[2] Cellular Telecommunications and Internet Association (CTIA), 2022, Test Plan for Wireless Device Over-the-Air Performance, Method of Measurement for Radiated RF Power and Receiver Performance (Version 4.0), 2022.

[3] Specification for Radio Disturbance and Immunity Measuring Apparatus and Methods - Part 1-4: Radio Disturbance and Immunity Measuring Apparatus - Antennas and Test Sites for Radiated Disturbance Measurements: CISPR 16-1-4, 2023.

[4] Wang F, Zhang C, Huang M, 2016, Smart Combination of Antenna Anechoic Chamber and EMC Anechoic Chamber. Safety and Electromagnetic Compatibility, 2016(5): 83–85.

[5] Wu C, Yu F, Luo Y, 2011, Construction of Dual-Purpose Anechoic Chamber. Safety and Electromagnetic Compatibility, 2011(2): 51–55.

[6] Analysis of Wireless Terminal Anechoic Chamber Ripple Measurement in CTIA OTA Accreditation. Journal of Microwaves, 2018(5): 73–78.

[7] Shen PH, Qi YH, Yu W, et al., 2021, UE Reporting Uncertainty Analysis in Radiated Two-stage MIMO Measurements. IEEE Transactions on Antennas and Propagation, 69(12): 8808–8815.

[8] Chen QW, Chen X, 2021, WLAN MIMO Device Performance Evaluation Using Improved RTS Measurement. IEEE Transactions on Instrumentation and Measurement, 70: 1–8.

[9] Kristian K, Chen XM, Jan C, et al., 2013, On OTA Test in the Presence of Doppler Spreads in a Reverberation Chamber. IEEE Antennas and Wireless Propagation Letters, 12: 886–889.

[10] Gao Y, Abouda K, Huot-Marchand A, 2012, Bandgap Circuitry with High Immunity to Harsh EMC Disturbances, 2012 Asia-Pacific Symposium on Electromagnetic Compatibility.

[11] Chen XM, Tang JZ, Li T, et al., 2018, Reverberation Chambers for Over-the-Air Tests: An Overview of Two Decades of Research. IEEE Access, 6: 49129–49143.

[12] Tian ZH, Huang Y, Xu Q, 2017, Efficient Measurement Techniques on OTA Test in Reverberation Chamber, 2017 IEEE International Symposium on Antennas and Propagation & USNC/ URSI National Radio Science Meeting. San Diego: IEEE, 2017: 1855–1856.

[13] Jensen MA, Arnold MT, Arnold MD, et al., 2023, Reconfigurable Surfaces in Reverberation Chambers for Over-the-Air Mobile Device Testing, 2023 International Workshop on Antenna Technology (iWAT). Aalborg: IEEE, 2023: 1–4.

[14] Kyosti P, Nuutinen JP, Kolu J, et al., 2009, Channel Modelling for Radiated Testing of MIMO Capable Terminals, ICT Mobile Summit 2009. Santander: IEEE, 2009: 1–8.

[15] Kyosti P, Jamsa T, Nuutinen JP, 2012, Channel Modelling for Multiprobe Over-the-Air MIMO Testing. International Journal of Antennas and Propagation, 2012: 1–11.